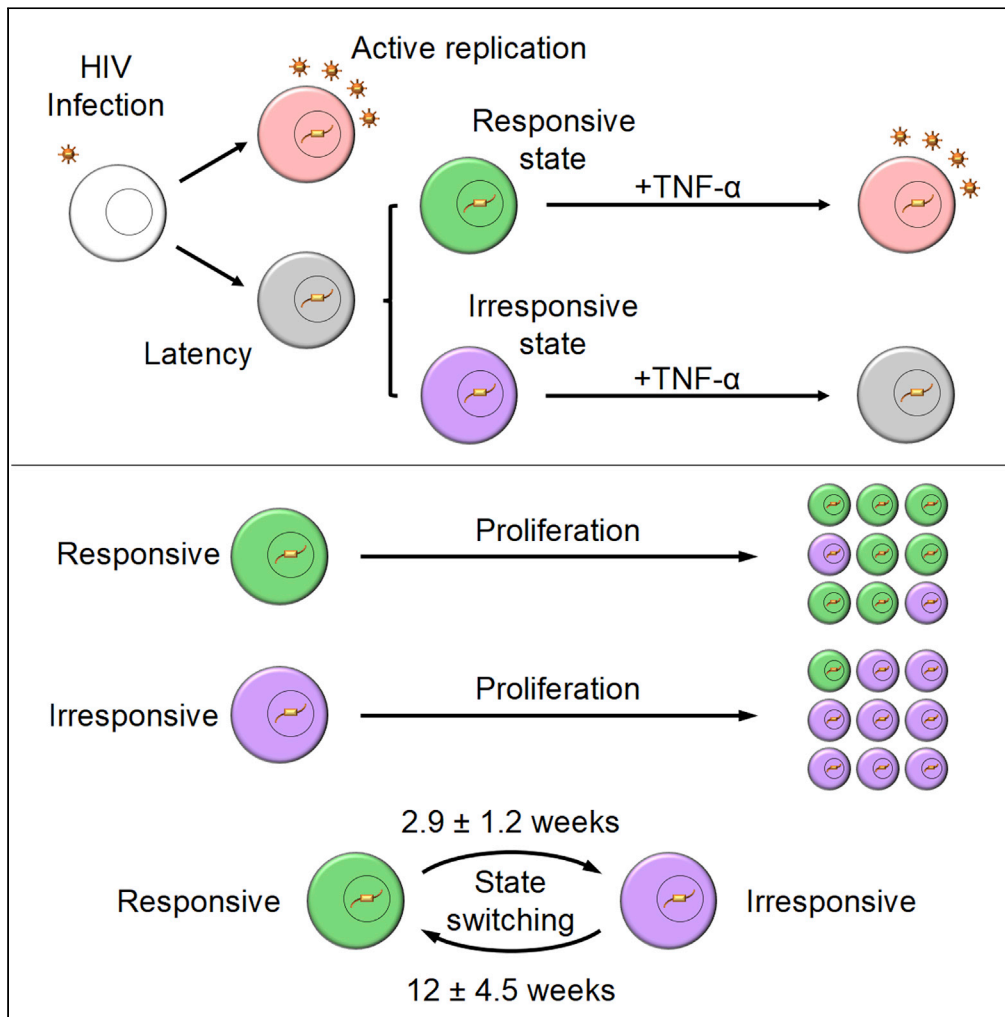## Article

A transient heritable memory regulates HIV reactivation from latency

Yiyang Lu, Harpal Singh, Abhyudai Singh, Roy D. Dar

absingh@udel.edu (A.S.)
roydar@illinois.edu (R.D.D.)

Highlights

Jurkat HIV latency model (JLat) shows inheritable responsiveness to TNF-α stimulation

JLat cells may switch between responsive state and irresponsive state spontaneously

Mathematical modeling indicates a memory timescale on the order of months

Article

A transient heritable memory regulates HIV reactivation from latency

Yiyang Lu,[1] Harpal Singh,[1] Abhyudai Singh,[2,*] and Roy D. Dar[1,3,4,5,*]

SUMMARY

Reactivation of human immunodeficiency virus 1 (HIV-1) from latently infected T cells is a critical barrier to cure patients. It remains unknown whether reactivation of individual latent cells occurs stochastically in response to latency reversal agents (LRAs) or is a deterministic outcome of an underlying cell state. To characterize these single-cell responses, we leverage the classical Luria-Delbrück fluctuation test where single cells are isolated from a clonal population and exposed to LRAs after colony expansion. Data show considerable colony-to-colony fluctuations with the fraction of reactivating cells following a skewed distribution. Modeling systematic measurements of fluctuations over time uncovers a transient heritable memory that regulates HIV-1 reactivation, where single cells are in an LRA-responsive state for a few weeks before switching back to an irresponsive state. These results have enormous implications for designing therapies to purge the latent reservoir and further utilize fluctuation-based assays to uncover hidden transient cellular states underlying phenotypic heterogeneity.

INTRODUCTION

With over 37 million infected individuals, human immunodeficiency virus 1 (HIV-1) remains a global epidemic of unprecedented proportions. Upon infection with HIV-1, CD4+ T cells may progress into a quiescent state called latency where they do not express viral genes and are capable of evading drug treatment. Latently infected cells can reactivate later and reinitiate active replication, causing a resurgence in viral levels if the patient goes off antiretroviral treatment (Figure 1A). The actively replicating virus hijacks the host-cell resources and machinery to create hundreds of viral progeny, lyse the cell, and spread to uninfected bystander cells (Weinberger et al., 2005, 2008). Thus HIV-1 latency remains the major barrier to a cure (Dahabieh et al., 2015; Richman et al., 2009; Ruelas and Greene, 2013; Siliciano and Greene, 2011; Sengupta and Siliciano, 2018). Several strategies exist to control and clear the latent reservoir of HIV-1 infected cells (Dahabieh et al., 2015; Richman et al., 2009; Ruelas and Greene, 2013). Much attention and research has focused on targeting the latent pool of cells with a small molecule treatment called the "shock and kill" strategy (Archin et al., 2012; Deeks, 2012; Rasmussen and Lewin, 2016). In this treatment, cells are reactivated from latency into an active state where they can then undergo killing by cytotoxic T cells and subsequently were cleared from the patient (Figure 1A) (Dahabieh et al., 2015). Unfortunately, "shock and kill" falls short owing to incomplete reactivation and killing of the latent reservoir (Cillo et al., 2014; Zerbato et al., 2019). Furthermore, latency reversal agents (LRAs) have been shown to impair cytotoxic T cell function (Shan et al., 2012; Jones et al., 2014, 2016), and clinical trials with histone deacetylase inhibitors (HDACis) and disulfiram, two classes of candidate LRAs, produced no major reduction in the size of the latent HIV-1 reservoir in patients on antiretroviral therapy (Rasmussen and Lewin, 2016). Alternatively, latency promoting agents have also been discovered that silence transcription of latent HIV-1 (Kessing et al., 2017, Dar et al., 2014, Lu et al., 2021), which points to the alternative "block and lock" strategy aiming to stabilize and prolong HIV-1 latency indefinitely.

Full control of the latent cell reservoir with small molecules, either by reactivation or silencing, requires a precise understanding of whether latent cells undergoing clonal expansion (Murray et al., 2016) have memory of their parent cell's responsiveness to treatments. In this context one can envision two different mechanisms of HIV-1 reactivation: (1) a random model where individual cells reactivate purely stochastically owing to noise in post-exposure signaling and viral gene expression (Singh et al., 2010; Singh and Weinberger, 2009; Dar et al., 2012; Burnett et al., 2009; Chavali et al., 2015); (2) an alternative heritable model where reactivation is a deterministic function of an underlying cell state (for example, HIV-1 promoter's

[1]Department of Bioengineering, University of Illinois at Urbana-Champaign, 321 Everitt Laboratory, 1406 West Green Street, Urbana, IL 61801, USA

[2]Department of Electrical and Computer Engineering, University of Delaware, Newark, DE 19716, USA

[3]Center for Biophysics and Quantitative Biology, University of Illinois at Urbana-Champaign, 1110 West Green Street, Urbana, IL 61801, USA

[4]Carl R. Woese Institute for Genomic Biology, University of Illinois at Urbana-Champaign, 1206 West Gregory Drive, Urbana, IL 61801, USA

[5]Lead contact

*Correspondence:
absingh@udel.edu (A.S.),
roydar@illinois.edu (R.D.D.)

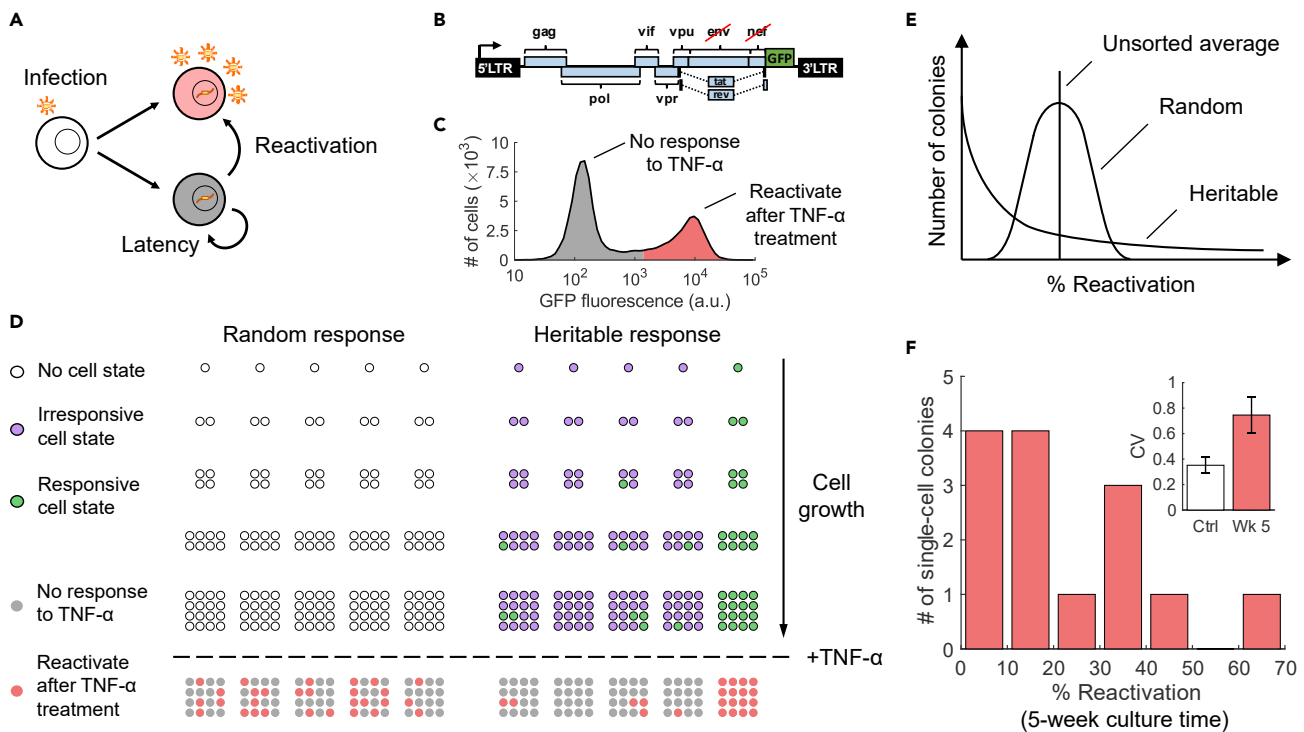https://doi.org/10.1016/j.isci.2021.102291

Figure 1. Heritable versus random reactivation response of HIV-1 latency to an external stimulus

(A) HIV-1 infection results in two phenotypes: active replication (red) where the infected cells produce new virions and latent infection (gray) where infected cells do not produce virions. Latently infected cells can reactivate and initiate virion production through cellular and environmental fluctuations.

(B) The cell line used in our investigation, the Jurkat latency model (JLat), is latently infected with a full-length HIV-1 gene circuit, with a deletion of *env* reading frame and a replacement of *nef* reading frame with a GFP element.

(C) Histogram of single-cell GFP fluorescence (measured with flow cytometry) from a JLat 9.2 bulk culture, after a 24-h tumor necrosis factor alpha (TNF-α) treatment. TNF-α is a potent activator of the HIV-1 LTR promoter and was administered at 10 ng/mL concentration. The histogram shows that there is a distinct bimodal distribution of response to TNF-α perturbation within a clonal population of JLat.

(D) We propose the following Luria-Delbrück experimental design to investigate if single-cell JLat response to TNF-α perturbation is random or heritable. A clonal population of JLat 9.2 was sorted into single cells using FACS and cultured individually into colonies. The colonies were subject to 10 ng/mL of TNF-α and the percentage of reactivated cells was measured using flow cytometry after 24 h of treatment. If JLat responds to TNF-α randomly, their responsiveness to TNF-α is determined at the time of TNF-α addition and thus would show low colony-to-colony variation. In contrast, if the response is heritable, then colony behaviors would be influenced by the parent cell resulting in large variations between colonies.

(E) The distribution of reactivation percentage would be centered on the unsorted average if the response is random, whereas the heritable model will result in a wide, skewed distribution for reactivation percentage across colonies.

(F) Histogram of reactivation percentage of 14 different JLat 9.2 colonies after a 24-h TNF-α treatment. Colonies were cultured for 5 weeks after FACS and were grown from single cells sorted from a bulk JLat 9.2 clonal population. The resulting distribution coincides with the heritable response prediction and confirms that JLat cells possess heritable memory of responsiveness to TNF-α perturbation. Inset: The noise in percent reactivation (quantified using the coefficient of variation CV) is significantly higher than the control noise floor as measured by fluctuations in percent reactivation across unsorted JLat populations ($p < 0.005$). Error bars in the inset represent the standard error of CV.

See also Figures S1 and S2.

epigenetic signature) just prior to LRA exposure. Despite its importance for understanding reactivation dynamics of the latent cell population, it is currently unknown which of the two cases, random response versus nonrandom heritable response, occurs in T cells latently infected with HIV-1.

To discriminate between the random versus heritable model we apply the Luria-Delbrück fluctuation test on a cell line model of HIV-1 latency (Figures 1B and 1C). More specifically, single cells are isolated from a clonal cell population having a single copy of the latent provirus at a unique integration site. Each single cell is expanded into a colony, and colony-to-colony fluctuations in the fraction of reactivating cells are quantified after LRA exposure (Figure 1D). In the random model, each individual cell has the same probability $\overline{p}$ of reactivation, in which case the number of reactivating cells follows a binomial distribution. A straightforward calculation shows that, for the random model, the colony-to-colony fluctuations in the fraction of

reactivating cells (as quantified using the coefficient of variation) is $\sqrt{\frac{1-\bar{p}}{N}}$, where N is the number of cells in the colony. Thus, for a sufficiently large N, the variations across colonies will be minimal, with each colony reactivating to the same frequency as the original clonal population. In the heritable model, the state of the single cell is propagated across generations, i.e., a more LRA-responsive single cell leads to a more responsive colony. This memory of the starting cell state in the expanded population drives considerable colony-to-colony fluctuations in the heritable model (Figure 1E). We develop a mathematical modeling framework to predict colony-to-colony differences for a transiently heritable cell state and systematically couple them to experimentally measured fluctuations to elucidate mechanisms regulating HIV-1 reactivation.

RESULTS

Responsiveness of HIV latency reversal to external stimulus displays heritability

To test which of the two types of response memory occurs in a latent cell population we utilized and cultured a known Jurkat latency model of HIV-1 (JLat, Figure 1B) (Jordan et al., 2003). This model consists of a Jurkat T cell population latently infected with a full-length HIV-1 construct. The construct contains a deletion of *env* and a replacement of *nef* reading frame with GFP. JLat 9.2, a clonal cell population with a single HIV-1 integration site, was selected for our experiments (Jordan et al., 2003). Tumor necrosis factor alpha (TNF-α) potently activates transcription of the HIV-1 LTR promoter through its nuclear factor κB binding sites (Malinin et al., 1997) and has been used for latency reversal assays on JLat cell lines in the previous literature at 10 ng/mL (Jordan et al., 2003; Bohn-Wippert et al., 2017; Dar et al., 2014). A typical response to TNF-α addition after 24h treatment is shown in Figure 1C. Here the bimodal distribution of identical cells shows a lower GFP peak of a cell subpopulation irresponsive to TNF-α and a higher GFP peak of cells that reactivate in response to TNF-α treatment (Figure 1C) (Weinberger et al., 2005, 2008). The percentage of reactivated cells measured using flow cytometry is quantified by the number of cells that turn on past a gating threshold divided by the total number of cells (Figures S2 and S3) and is ≈20% for JLat 9.2 at 10 ng/mL TNF-α induction.

To perform the Luria-Delbrück fluctuation test, we used fluorescence-activated cell sorting (FACS) to sort single cells into 96-well plates and grow out JLat single-cell colonies (transparent methods, Figure S1). Of the cells that survived and expanded, 14 JLat 9.2 single-cell colonies were grown out over 5 weeks and subsequently treated with TNF-α for 24 h to determine the fraction of reactivating cells (% reactivation) (transparent methods, Figure S2). It is intriguing that the data reveal a skewed distribution for the % reactivation across colonies (Figure 1F) with a high coefficient of variation (CV) of ≈0.75. The parent JLat 9.2 population shows a 20% reactivation, whereas 4 of 14 single-cell colonies reactivate less than 10% and 2 colonies reactivate greater than 40%. The skewed distribution observed at week 5 closely resembles one expected from a nonrandom heritable response model (Figures 1E and 1F). Next, we quantified the biological lower limit of noise in this assay, by measuring the % reactivation in unsorted JLat 9.2 populations over an 8-week period (Figure 2A, black dots). The CV of week-to-week fluctuations in these unsorted populations was determined to be ≈ 0.35 and represents the control noise floor of the fluctuation test. The significantly higher fluctuations in the % reactivation across single-cell colonies (CV ≈ 0.75) as compared with the control noise floor (Figure 1F; inset, p < 0.005) rules out the random response model but is consistent with a heritable cell state regulating cellular responsiveness to TNF-α.

The cell outgrowth assay followed by activator treatment reveals that JLat 9.2 cells exhibit nonrandom heritable memory with respect to TNF-α activation. If the cell state dictating HIV-1 reactivation is transient, then the fluctuations in the % reactivation should decay over time and reach the noise floor. To determine the timescale of this noise relaxation, we measured TNF-α response across 16 single-cell colonies (14 colonies at week 5 plus 2 additional colonies that grew at week 7) every 2 weeks starting from week 5 (Figure 2A). The low number of colonies is due to the limited survivability after single-cell FACS of Jurkat cells; of 384 sorted single cells, only 16 were able to proliferate into colonies. The reactivation level of the parental unsorted JLat 9.2 cell population was acquired to compare colony reactivation with unsorted reactivation. In brief, the unsorted JLat 9.2 population was cultured in duplicate and cells were measured by flow cytometry every 2 weeks after 24-h TNF-α treatments. For each time point, the mean of two JLat 9.2 unsorted populations was acquired. Unsorted % reactivation drifted from about 32% in week 5 to about 12% in week 13 (black dots, Figure 2A). The difference between each colony-wise % reactivation and the unsorted (Δ% Reactivation) decreased as culture time went on (Figures 2B and 2C). As expected for a transiently heritable cell state, the colony-to-colony fluctuations in the % reactivation attenuate over time, starting from a wide, skewed distribution at week 5, to a narrow distribution at week
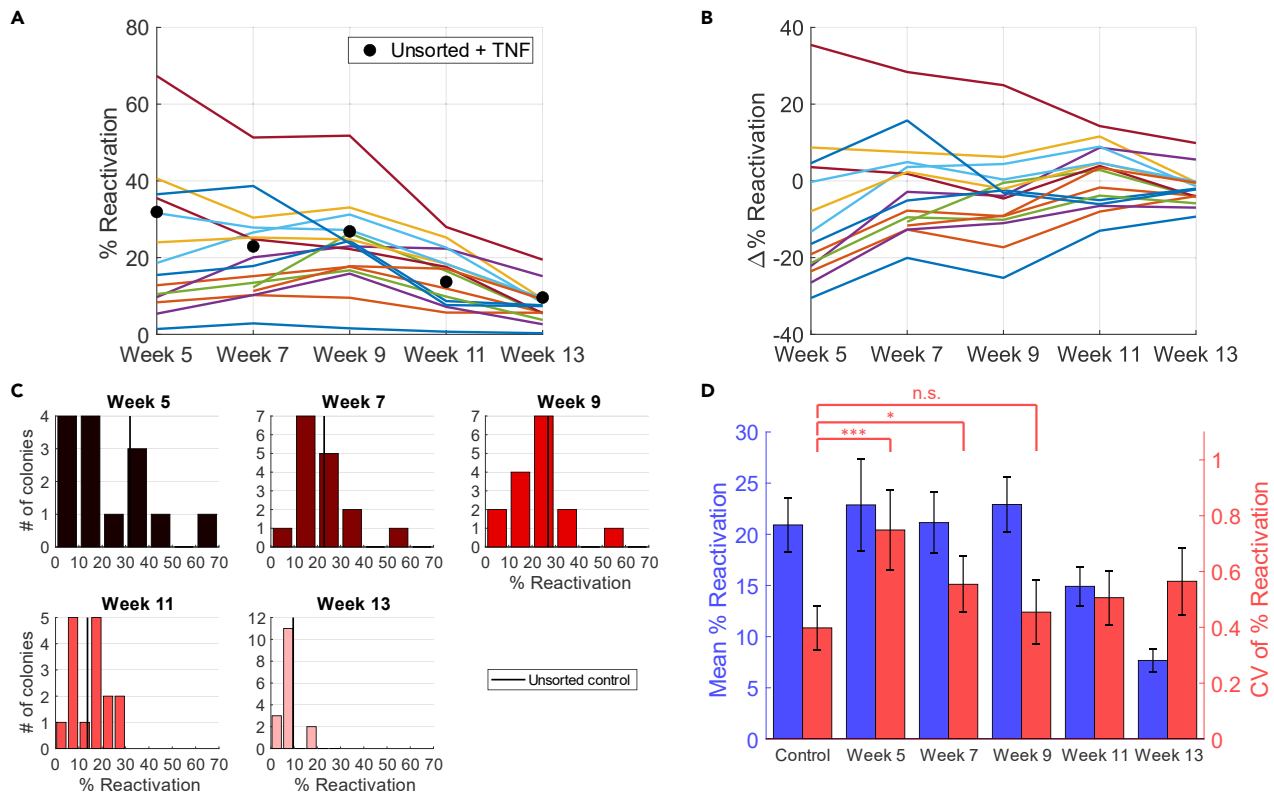
Figure 2. Experimental results from long-term culturing of single-cell JLat colonies reveal a transient heritable response to TNF-α perturbation

(A and B) (A) Reactivation percentage of each colony across weeks 5–13 after TNF-α exposure of 24 h, tested biweekly. Two colonies did not reach experimentally feasible concentrations at week 5 and were included starting from week 7. Black dots represent the control values, measured by exposing the unsorted culture to the same TNF-α treatment for 24 h. The colonies gradually moved closer toward the unsorted control as culturing time progressed. This trend is more clearly represented in (B) where the difference in reactivation percentage between each colony and the control, Δ% Reactivation, is visualized. The approach toward unsorted control is demonstrated by the bundling of colony-wise response around 0 at later time points.

(C) Histogram of reactivation percentage of single-cell colonies from each week's measurement. Week 5 has a total of 14 colonies, whereas the remaining weeks have 16. Unsorted control average is shown as black vertical lines. Bin size for weeks 5, 7, and 9 was set to 10, whereas for weeks 11 and 13 it was set to 5 for better resolution. The histograms also show the convergence of colony-wise behavior toward the unsorted control.

(D) Bar plot of the colony-wise mean reactivation percentage (blue) and colony-wise mean CV (coefficient of variation squared) of reactivation percentage (red). Mean % reactivation values showed an overall decreasing trend as culture time went on, whereas mean CV of % reactivation decreased for the first 5 weeks before reaching a plateau in weeks 11 and 13. The control value is a pooled average of all unsorted + TNF-α treatment values across the 5 time points. Bar heights and error bars represent bootstrapped mean and standard error. Levels of significance are indicated as n.s. ($p \geq 0.1$), one star (*, $0.1 > p \geq 0.05$) or three stars (***, $p < 0.01$). p Values were calculated using bootstrapping. See transparent methods for details on statistics.

See also Figures S5–S7 for alternative gating strategies.

13 (Figure 2C). The CV of the % reactivation at weeks 5 and 7 is significantly higher than the control noise floor but drops to the noise floor starting from week 9. As also observed in the unsorted populations, the mean % reactivation from week 11 and week 13 are significantly lower than the control mean ($p < 0.05$ and $p < 0.01$ respectively), whereas weeks 5–9 do not show significant changes compared with the control (Figure 2D). Careful analysis shows that the results of Figure 2 are insensitive to the gating strategy used (transparent methods, Figures S5–S7).

Mathematical modeling of the transient heritable memory

To systematically characterize the hidden memory regulating HIV reactivation from the fluctuation test data, we developed a mathematical model of clonal expansion where single cells switch between an irresponsive and responsive state (Figure 3A). The states are transiently heritable, i.e., the state is inherited for some generations before it is lost (Figure 2A and transparent methods, Figure S3). Let $p(t)$ denote the reactivation probability of an individual cell at time t, and is assumed to switch between two values: $p(t) = 0$ (irresponsive state) and $p(t) = 1$ (fully responsive state). Cells in the irresponsive state become
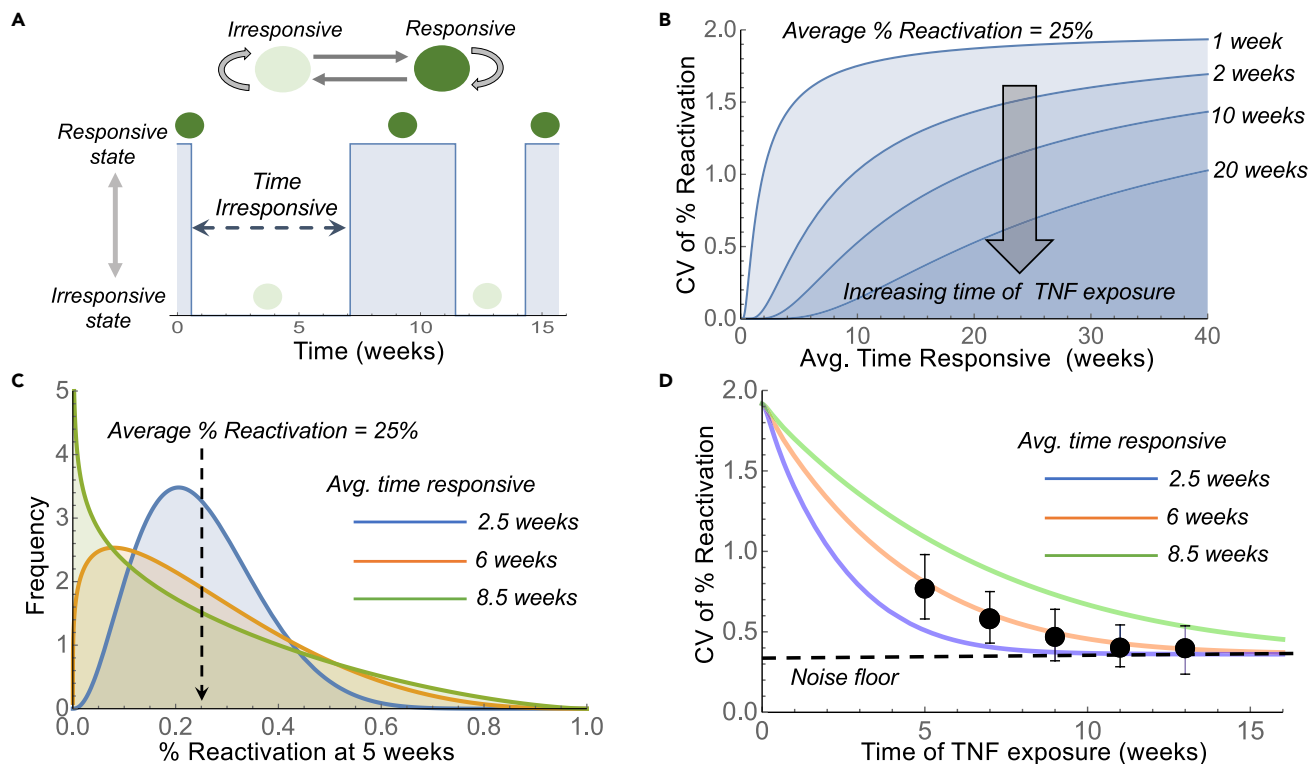
Figure 3. A transient cell state governs HIV-1 exit from latency

(A) Schematic of the stochastic model where prior to TNF-α exposure, individual cells reversibly switch between a TNF-α irresponsive and a responsive state. Self arrows represent proliferation of cells with the mother cell state being inherited by daughters. A sample realization of cells switching states over time is shown below.

(B) The predicted colony-to-colony fluctuations in the fraction of reactivating cells (as measured by the coefficient of variation CV) increases for longer periods in the responsive state assuming a fixed 25% reactivation averaged across colonies. Plots are shown for different times of TNF-α exposure.

(C) Predicted distribution of the fraction of reactivating cells across colonies after 5 weeks of growth for different average times in the responsive state. Distributions are obtained by using a beta distribution with an average 25% reactivation and noise as given by Equation (2).

(D) Measured colony-to-colony fluctuations (with error bars showing standard error) starting from 5 to 13 weeks (black circles corresponding to data from Figure 2D). The fluctuations are considerably high at the initial 5-week time point (CV = 75%) and then gradually decrease to the noise floor. Note that the 11- and 13-week timepoints have been corrected for the mean as discussed in the main text. Model predicted CV as per Equation Equation (4) are shown assuming a noise floor $CV_{NF} = 0.35$ for different average times in the responsive state.

See also Figures S3 and S4.

responsive with rate k, and responsive cells become irresponsive with rate γ. In the stochastic formulation of the model, the time spent in responsive and irresponsive states is exponentially distributed with means $1/\gamma$ and $1/k$, respectively. These switching rates yield the following steady-state mean and noise levels of $p(t)$ (see transparent methods for details on model description and analysis):

$$\overline{p} \equiv \lim_{t \to \infty} \langle p(t) \rangle = \frac{k}{k+\gamma}; \quad CV_p^2 \equiv \lim_{t \to \infty} \frac{\langle p^2(t) \rangle - \langle p(t) \rangle^2}{\langle p(t) \rangle^2} = \frac{1-\overline{p}}{\overline{p}} \qquad \text{(Equation 1)}$$

where the angular brackets p denote the expected value and $\overline{p}$ is the fraction of responsive cells in the original unsorted population.

Having defined stochastic transitions between the two cell states, we next model the clonal expansion in the Luria-Delbrück experiment. A single cell is chosen from the original population at time $t = 0$, and this initial cell is either in the responsive state with probability $\overline{p}$ or in the irresponsive state with probability $1 - \overline{p}$. Starting from a single cell, colony size increases exponentially over time with cell-doubling times assumed to be the same irrespective of the underlying state (transparent methods, Figure S4). As the lineage expands, single cells reversibly switch between states and the mother cell state is inherited by both

daughters upon mitosis. Considering exposure to TNF-α at time *t*, our analysis predicts the CV of the colony-to-colony fluctuations in % reactivation

$$CV(t) = CV_p e^{-(\gamma + k)t}$$ (Equation 2)

to decay exponentially with rate *k*+γ (see transparent methods for details). Note that, if reactivation is done at *t = 0*, then

$$CV(0) = CV_p = \sqrt{\frac{1 - \overline{p}}{\overline{p}}}$$ (Equation 3)

is consistent with the Bernoulli reactivation outcome for the initial cell. Considering $\overline{p} \approx 20\%$ responsive cells in the original population, this would correspond to $CV(0) \approx 2$. As expected, colony-to-colony fluctuations are high when the reactivation is done early in the lineage expansion as the memory of the initial cell is retained. Over time, these fluctuations decay to zero with each colony equilibrating to the same steady-state % reactivation $\overline{p}$. For a fixed time of TNF-α exposure, colony-to-colony fluctuations are enhanced by slower switching between states (Figures 3B and 3C).

For fitting the predicted *CV* to data, we modify (2)

$$CV(t) = \sqrt{CV_p^2 e^{-2(\gamma + k)t} + CV_{NF}^2}$$ (Equation 4)

to include a noise floor CV_{NF}^2 as quantified using fluctuations in % reactivation across unsorted populations. Given an a priori knowledge of, fitting (4) to experimentally measured colony-to-colony fluctuations at different times of exposure infers the decay rate *k*+γ. Note from (1) that $\overline{p}$ itself is determined by the ratio of *k* and γ. Thus, combining knowledge of both $\overline{p}$ with the inferred decay rate allows both switching rates to be uniquely estimated. Before fitting (4) to the measured colony-to-colony fluctuations, recall that the average % reactivation of single-cell colonies was significantly reduced at week 11 and week 13 (Figure 2D). For this reason, the measured CV in % reactivation at these time points is likely higher than if the mean % reactivation had remained constant at 20%. Assuming CV^2 to be inversely proportional to the mean % reactivation (as in a binomial distribution), we readjust the CV values at weeks 11 and 13 assuming a 20% mean reactivation. An alternative approach is to simply exclude data points at weeks 11 and 13, and both approaches yield statistically similar parameter estimates. Fitting model-predicted CV to measured fluctuations reveals the noise decay rate *k*+γ to be 0.24 ± 0.1 per week (Figure 3D) where the ± denotes the 95% confidence interval as estimated using bootstrapping. Based on a $\overline{p} \approx 20\%$, this corresponds to single cells being in the response state for 6.3 ± 2.6 weeks. A key assumption in this calculation is that sorted single cells can instantly start proliferating. However, the stress of single-cell sorting can create a lag phase before sorted cells can execute normal cellular proliferation. A quick analysis based on cell densities at different times of the colony expansion points to a lag phase of around 2–3 weeks (see details in the supplementary information), and accounting for this delay, reduces the average time cells stay in the response state to be 2.9 ± 1.2 weeks. Given that only 20% of cells are TNF-α responsive yields the average time a cell is in the irresponsive state to be 12 ± 4.5 weeks.

DISCUSSION

The Luria-Delbrück experiment, also called the "Fluctuation Test," introduced over 75 years ago, demonstrated that genetic mutations arise randomly in the absence of selection—rather than in response to selection—and led to a Nobel Prize (Luria and Delbruck, 1943). Combining this classical fluctuation test with mathematical modeling we have developed a novel methodology to infer timescales of reversible switching between cellular states that exist within the same clonal population. In essence, slower switching rates lead to higher colony-to-colony fluctuations in the assayed phenotype (for example, the % HIV-1 reactivation across colonies) (Figures 3B and 3C). The key advantage of this method is that it is general enough to be applied to any proliferating cell type and only involves making a single endpoint measurement. This is especially important for scenarios where a measurement involves killing the cell, and hence the state of the same cell cannot be measured at different time points. Along these lines, the fluctuation test has had tremendous recent success in deciphering stochastic transitions between drug-tolerant states underlying cancer drug resistance, where drug exposure leads to heterogeneous single-cell responses between cell death and survival (Shaffer et al., 2017, 2019).

We leveraged the fluctuation test to address a fundamental question in HIV-1 latency: is the reactivation of the latent provirus upon LRA exposure purely stochastic or a deterministic function of an underlying cell

state (Figure 1D). Using the Jurkat T cell line model of HIV-1 latency (JLat 9.2), containing a modified full-length provirus that expresses GFP upon reactivation (Figures 1B and 1C) (Jordan et al., 2003), the fluctuation data strongly point to the heritable model—cells switch between responsive and irresponsive states, and the cell state at the time of TNF-α exposure determines the all-or-none reactivation decision. Remarkably, these states are transiently inherited across generations with a timescale of months (Figure 3D). This point is exemplified by the fact that even after 5 weeks of clonal expansion there are significant colony-to-colony differences in TNF-α responsiveness (Figure 1F) and these differences attenuate over time to baseline levels at $\approx$ 10 weeks (Figure 2D). Although we were able to distinguish between random and heritable response for the Jurkat latency model of HIV-1, systems following the heritable model but with switching rates exceeding the sampling rate of our experimental design will impose difficulties in this task and would require more advanced techniques to tease out the details. Despite focusing on JLat 9.2, a single JLat clonal integration site, we predict that the heritable model is conserved across integrations but with different timescales (Pearson et al., 2008). The long timescales of switching involved here imply epigenetic mechanisms at play, and indeed, prior work has shown that DNA methylation patterns at the HIV promoter critically regulate provirus reactivation (Kauder et al., 2009; Blazkova et al., 2009; Bednarik et al., 1990). Moreover, RNA-induced epigenetic silencing using promoter-targeted shRNAs has been shown to suppress HIV-1 reactivation from latency in JLat 9.2 cells (Mendez et al., 2018). Of interest, recently constructed high-resolution maps of histone marks in human cells reveal stochastic switching between fully methylated and unmethylated states of DNA at several gene loci (Onuchic et al., 2018). Taken together, these results suggest that dynamic, but slow, turnovers of epigenetic signatures at the HIV-1 promoter may provide a mechanism for switching between LRA-responsive and irresponsive states.

The measured colony-to-colony fluctuations in the fraction of reactivating cells over time reveals that cells can remain irresponsive to TNF-α for several months before switching to a responsive state. Cells in the responsive state return to become irresponsive after a few weeks. This result has important implications for designing therapies to purge the latent reservoir (Deeks, 2012; Spina et al., 2013; Shirakawa et al., 2013) and suggests that a strategy with multiple LRA treatments spaced over several months may be more effective than single-round, single-LRA treatments (Ho et al., 2013; Dar et al., 2014; Xing and Siliciano, 2013). Consistent with the idea, previous work has shown that periodic treatments can reactivate more latent virus (Ho et al., 2013). While this contribution has focused on HIV-1 reactivation in Jurkat T-cells using TNF-α induction, it raises intriguing questions on the generality of transient memory states in the context of other LRAs and cell types. For example, fluctuation-based assays can be done at different proviral integration sites in Jurkat T-cells, at different TNF-α dosage, in other cell types (for example, myeloid models of HIV-1 latency), and, most importantly, using a variety of other LRAs, such as HDAC inhibitors (Archin et al., 2012; Shirakawa et al., 2013; Manson Mcmanamy et al., 2014), synergistic combinations of PKC agonists (Williams et al., 2004), DNA cytosine methylation inhibitor 5-aza-2'deoxycytidine (Blazkova et al., 2009; Kauder et al., 2009), and many others reported in the literature. Such studies will be essential to decipher cell-state signatures in the latent reservoir that will guide efforts for HIV-1 treatment. Alternatively, the finding that cells can remain irresponsive to TNF-α for several months before switching to a responsive state may also have implications for additional treatment strategies. The "block and lock" strategy involves silencing HIV-1 expression into a prolonged latent state (Vansant et al., 2020; Kessing et al., 2017). If the responsiveness of HIV-1 to silencing drugs is governed by the same principle, the responsiveness timescale quantified here may guide the treatment design needed for latency promoting agent administration, in both composition and timing.

Limitations of the study

This study includes two limitations related to HIV virology. First, the downside of throughput limitations in the growth and handling of clonal populations limited this study to a single integration site. Further research covering a broad spectrum of HIV viral integration sites will provide a range of transient memory timescales that are closer to the *in vivo* setting. Second, the fluctuation test required the isolation and growth of individual cells isolated from a clonal Jurkat latency model of HIV. Ideally, this experiment would be performed on a primary cell model of latency but resting CD4+ T cells expansion is limited to very slow homeostatic proliferation, which may prove challenging for setting up such an experiment.

Resource availability

Lead contact

Further information and requests for resources and reagents should be directed to and will be fulfilled by the lead contact, Roy Dar (roydar@illinois.edu).

Materials availability

This study did not generate new unique reagents.

Data and code availability

This study did not generate/analyze datasets/code.

METHODS

All methods can be found in the accompanying transparent methods supplemental file.

SUPPLEMENTAL INFORMATION

Supplemental information can be found online at https://doi.org/10.1016/j.isci.2021.102291.

REFERENCES

Archin, N.M., Liberty, A.L., Kashuba, A.D., Choudhary, S.K., Kuruc, J.D., Crooks, A.M., Parker, D.C., Anderson, E.M., Kearney, M.F., Strain, M.C., et al. (2012). Administration of vorinostat disrupts HIV-1 latency in patients on antiretroviral therapy. Nature *487*, 482–485.

Bednarik, D.P., Cook, J.A., and Pitha, P.M. (1990). Inactivation of the HIV LTR by DNA CpG methylation: evidence for a role in latency. EMBO J. *9*, 1157–1164.

Blazkova, J., Trejbalova, K., Gondois-Rey, F., Halfon, P., Philibert, P., Guiguen, A., Verdin, E., Olive, D., Van Lint, C., Hejnar, J., and Hirsch, I. (2009). CpG methylation controls reactivation of HIV from latency. PLoS Pathog. *5*, e1000554.

Bohn-Wippert, K., Tevonian, E.N., Megaridis, M.R., and Dar, R.D. (2017). Similarity in viral and host promoters couples viral reactivation with host cell migration. Nat. Commun. *8*, 15006.

Burnett, J.C., Miller-Jensen, K., Shah, P.S., Arkin, A.P., and Schaffer, D.V. (2009). Control of stochastic gene expression by host factors at the HIV promoter. PLoS Pathog. *5*, e1000260.

Chavali, A.K., Wong, V.C., and Miller-Jensen, K. (2015). Distinct promoter activation mechanisms modulate noise-driven HIV gene expression. Sci. Rep. *5*, 17661.

Cillo, A.R., Sobolewski, M.D., Bosch, R.J., Fyne, E., Piatak, M., Jr., Coffin, J.M., and Mellors, J.W. (2014). Quantification of HIV-1 latency reversal in resting CD4+ T cells from patients on suppressive antiretroviral therapy. Proc. Natl. Acad. Sci. U S A *111*, 7078–7083.

Dahabieh, M.S., Battivelli, E., and Verdin, E. (2015). Understanding HIV latency: the road to an HIV cure. Annu. Rev. Med. *66*, 407–421.

Dar, R.D., Hosmane, N.N., Arkin, M.R., Siliciano, R.F., and Weinberger, L.S. (2014). Screening for noise in gene expression identifies drug synergies. Science *344*, 1392–1396.

Dar, R.D., Razooky, B.S., Singh, A., Trimeloni, T.V., Mccollum, J.M., Cox, C.D., Simpson, M.L., and Weinberger, L.S. (2012). Transcriptional burst frequency and burst size are equally modulated across the human genome. Proc. Natl. Acad. Sci. U S A *109*, 17454–17459.

Deeks, S.G. (2012). HIV: shock and kill. Nature *487*, 439–440.

Ho, Y.C., Shan, L., Hosmane, N.N., Wang, J., Laskey, S.B., Rosenbloom, D.I., Lai, J., Blankson, J.N., Siliciano, J.D., and Siliciano, R.F. (2013). Replication-competent noninduced proviruses in the latent reservoir increase barrier to HIV-1 cure. Cell *155*, 540–551.

Jones, R.B., Mueller, S., O'connor, R., Rimpel, K., Sloan, D.D., Karel, D., Wong, H.C., Jeng, E.K., Thomas, A.S., Whitney, J.B., et al. (2016). A subset of latency-reversing agents expose HIV-infected resting CD4+ T-cells to recognition by cytotoxic T-lymphocytes. PLoS Pathog. *12*, e1005545.

Jones, R.B., O'connor, R., Mueller, S., Foley, M., Szeto, G.L., Karel, D., Lichterfeld, M., Kovacs, C., Ostrowski, M.A., Trocha, A., et al. (2014). Histone deacetylase inhibitors impair the elimination of HIV-infected cells by cytotoxic T-lymphocytes. PLoS Pathog. *10*, e1004287.

Jordan, A., Bisgrove, D., and Verdin, E. (2003). HIV reproducibly establishes a latent infection after acute infection of T cells in vitro. EMBO J. *22*, 1868–1877.

Kauder, S.E., Bosque, A., Lindqvist, A., Planelles, V., and Verdin, E. (2009). Epigenetic regulation of HIV-1 latency by cytosine methylation. PLoS Pathog. *5*, e1000495.

Kessing, C.F., Nixon, C.C., Li, C., Tsai, P., Takata, H., Mousseau, G., Ho, P.T., Honeycutt, J.B., Fallahi, M., Trautmann, L., et al. (2017). In vivo suppression of HIV rebound by didehydro-cortistatin A, a "Block-and-Lock" strategy for HIV-1 treatment. Cell Rep. *21*, 600–611.

Lu, Y., Bohn-Wippert, K., Pazerunas, P.J., Moy, J.M., Singh, H., and Dar, R.D. (2021). Screening for gene expression fluctuations reveals latency promoting agents of HIV. Proc. Natl. Acad. Sci. U.S.A. 118 (11), e2012191118.

Luria, S.E., and Delbruck, M. (1943). Mutations of bacteria from virus sensitivity to virus resistance. Genetics 28, 491–511.

Malinin, N.L., Boldin, M.P., Andrei, K.V., and Wallach, D. (1997). MAP3K-related kinase involved in NF-KB induction by TNF, CD95 and IL-1. Nature 385, 540–544.

Manson Mcmanamy, M.E., Hakre, S., Verdin, E.M., and Margolis, D.M. (2014). Therapy for latent HIV-1 infection: the role of histone deacetylase inhibitors. Antivir. Chem. Chemother. 23, 145–149.

Mendez, C., Ledger, S., Petoumenos, K., Ahlenstiel, C., and Kelleher, A.D. (2018). RNA-induced epigenetic silencing inhibits HIV-1 reactivation from latency. Retrovirology 15, 67.

Murray, A.J., Kwon, K.J., Farber, D.L., and Siliciano, R.F. (2016). The latent reservoir for HIV-1: how immunologic memory and clonal expansion contribute to HIV-1 persistence. J. Immunol. 197, 407–417.

Onuchic, V., Lurie, E., Carrero, I., Pawliczek, P., Patel, R.Y., Rozowsky, J., Galeev, T., Huang, Z., Altshuler, R.C., Zhang, Z., et al. (2018). Allele-specific epigenome maps reveal sequence-dependent stochastic switching at regulatory loci. Science 361, eaar3146.

Pearson, R., Kim, Y.K., Hokello, J., Lassen, K., Friedman, J., Tyagi, M., and Karn, J. (2008). Epigenetic silencing of human immunodeficiency virus (HIV) transcription by formation of restrictive chromatin structures at the viral long terminal repeat drives the progressive entry of HIV into latency. J. Virol. 82, 12291–12303.

Rasmussen, T.A., and Lewin, S.R. (2016). Shocking HIV out of hiding: where are we with clinical trials of latency reversing agents? Curr. Opin. HIV AIDS 11, 394–401.

Richman, D.D., Margolis, D.M., Delaney, M., Greene, W.C., Hazuda, D., and Pomerantz, R.J. (2009). The challenge of finding a cure for HIV infection. Science 323, 1304–1307.

Ruelas, D.S., and Greene, W.C. (2013). An integrated overview of HIV-1 latency. Cell 155, 519–529.

Sengupta, S., and Siliciano, R.F. (2018). Targeting the latent reservoir for HIV-1. Immunity 48, 872–895.

Shaffer, S.M., Dunagin, M.C., Torborg, S.R., Torre, E.A., Emert, B., Krepler, C., Beqiri, M., Sproesser, K., Brafford, P.A., Xiao, M., et al. (2017). Rare cell variability and drug-induced reprogramming as a mode of cancer drug resistance. Nature 546, 431–435.

Shaffer, S.M., Emert, B.L., Reyes-Hueros, R., Cot, C., Harmange, G., Sizemore, A.E., Gupte, R., Torre, E., Singh, A., Bassett, D.S., and Raj, A. (2019). Memory sequencing reveals heritable single cell gene expression programs associated with distinct cellular behaviors. bioRxiv, 379016.

Shan, L., Deng, K., Shroff, N.S., Durand, C.M., Rabi, S.A., Yang, H.C., Zhang, H., Margolick, J.B., Blankson, J.N., and Siliciano, R.F. (2012). Stimulation of HIV-1-specific cytolytic T lymphocytes facilitates elimination of latent viral reservoir after virus reactivation. Immunity 36, 491–501.

Shirakawa, K., Chavez, L., Hakre, S., Calvanese, V., and Verdin, E. (2013). Reactivation of latent HIV by histone deacetylase inhibitors. Trends Microbiol. 21, 277–285.

Siliciano, R.F., and Greene, W.C. (2011). HIV latency. Cold Spring Harb. Perspect. Med. 1, a007096.

Singh, A., Razooky, B., Cox, C.D., Simpson, M.L., and Weinberger, L.S. (2010). Transcriptional bursting from the HIV-1 promoter is a significant source of stochastic noise in HIV-1 gene expression. Biophysical J. 98, L32–L34.

Singh, A., and Weinberger, L.S. (2009). Stochastic gene expression as a molecular switch for viral latency. Curr. Opin. Microbiol. 12, 460–466.

Spina, C.A., Anderson, J., Archin, N.M., Bosque, A., Chan, J., Famiglietti, M., Greene, W.C., Kashuba, A., Lewin, S.R., Margolis, D.M., et al. (2013). An in-depth comparison of latent HIV-1 reactivation in multiple cell model systems and resting CD4+ T cells from aviremic patients. PLoS Pathog. 9, e1003834.

Vansant, G., Bruggemans, A., Janssens, J., and Debyser, Z. (2020). Block-and-lock strategies to cure HIV infection. Viruses 12, 84.

Weinberger, L.S., Burnett, J.C., Toettcher, J.E., Arkin, A.P., and Schaffer, D.V. (2005). Stochastic gene expression in a lentiviral positive-feedback loop: HIV-1 Tat fluctuations drive phenotypic diversity. Cell 122, 169–182.

Weinberger, L.S., Dar, R.D., and Simpson, M.L. (2008). Transient-mediated fate determination in a transcriptional circuit of HIV. Nat. Genet. 40, 466–470.

Williams, S.A., Chen, L.F., Kwon, H., Fenard, D., Bisgrove, D., Verdin, E., and Greene, W.C. (2004). Prostratin antagonizes HIV latency by activating NF-kappaB. J. Biol. Chem. 279, 42008–42017.

Xing, S., and Siliciano, R.F. (2013). Targeting HIV latency: pharmacologic strategies toward eradication. Drug Discov. Today 18, 541–551.

Zerbato, J.M., Purves, H.V., Lewin, S.R., and Rasmussen, T.A. (2019). Between a shock and a hard place: challenges and developments in HIV latency reversal. Curr. Opin. Virol. 38, 1–9.

Supplemental information

A transient heritable memory regulates

HIV reactivation from latency

Yiyang Lu, Harpal Singh, Abhyudai Singh, and Roy D. Dar
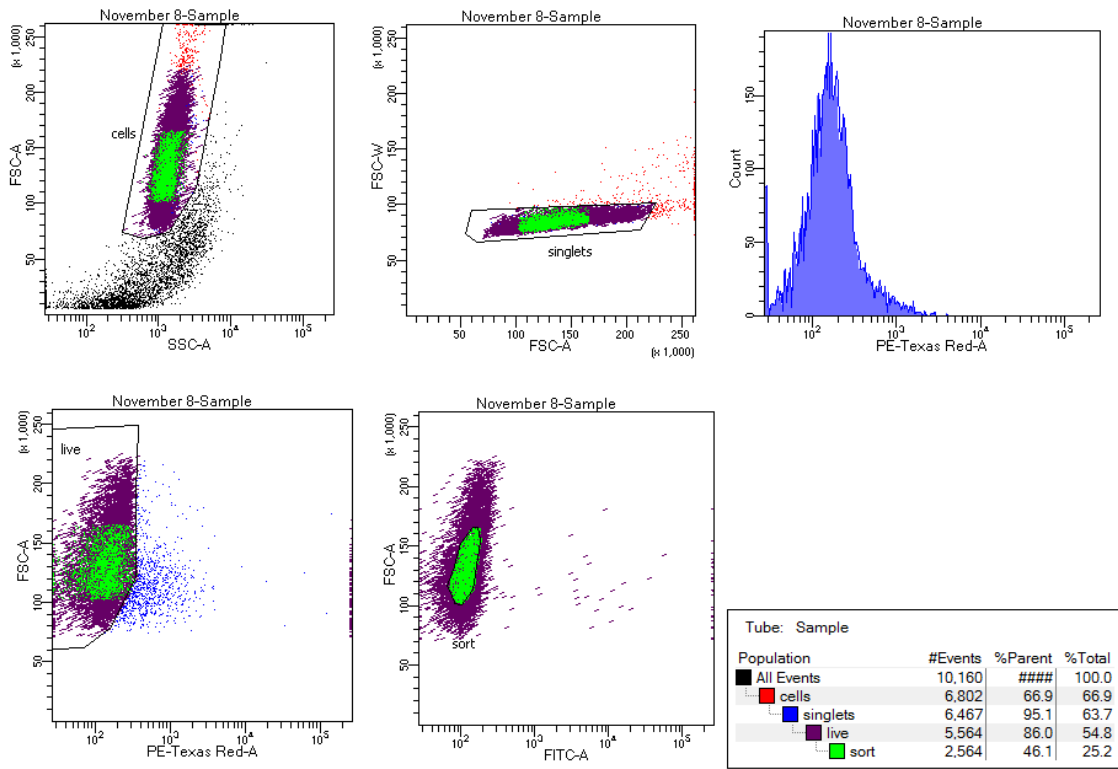
Figure S1. Gating strategy during single-cell sorting of JLat 9.2, Related to Figure 1.
Propidium iodide (PI) staining was used to distinguish live cells from dead ones. Four layers of gating were implemented during the sorting. The first layer ("cells" gate) gets rid of debris and dead cells. The second layer ("singlets" gate) removes large particles and ensures every cell passes through is a singlet. The third layer ("live" gate) selects cells with low fluorescence in the PE-Texas Red channel, which captures PI fluorescence, and removes dead cells. The final gate ("sort" gate) only includes the center of the live cell distribution and selects cells that are representative of the population behavior. The cells in the "sort" gate were plated onto 96-well plates, with one cell in each well. Pairs of diagonal double dots represent single cells and is only used to ease visualization when the cell density is low in certain regions of the axes.
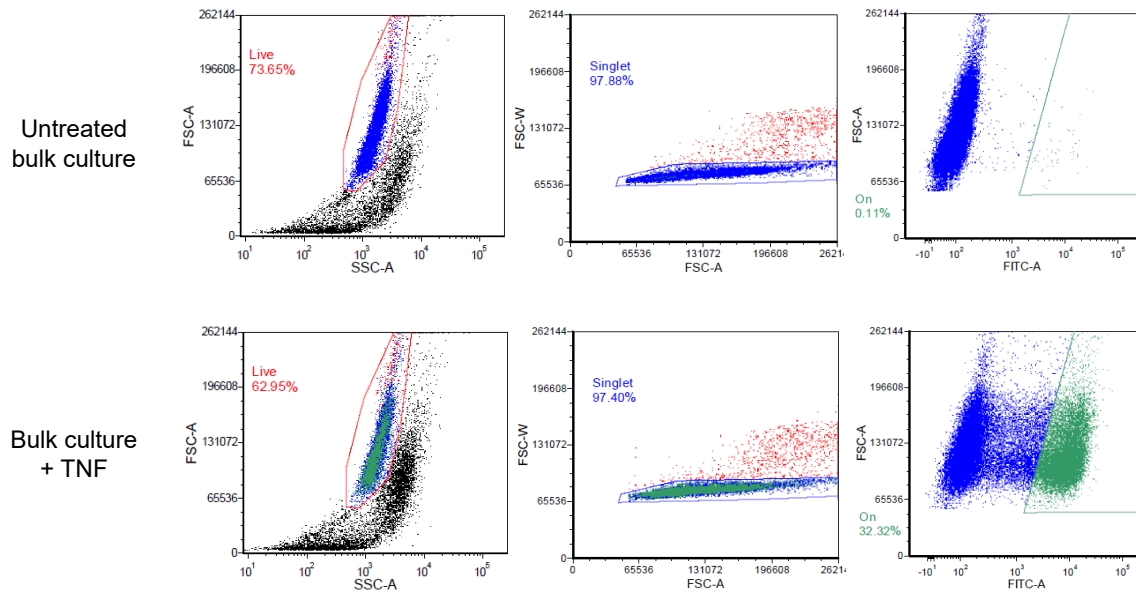
Figure S2. Gating strategy for latency reversal assay, Related to Figure 1. We used a three-layered gating to quantify the reactivation percentage of JLat 9.2. Shown here is a sample gating for untreated bulk culture (top row) and bulk culture after 24 hours of TNF treatment (bottom row). The first layer ("Live" gate) gets rid of debris and dead cells. The second layer ("Singlet" gate) gets rid of large cells that are potentially doublets. The third layer ("On" gate) only includes cells with significantly higher fluorescence in FITC channel, which captures GFP fluorescence. The ratio of number of cells in the "On" gate (green dots) over the number of all cells in the "Singlet" gate (green + blue dots) were used as the quantification of reactivation percentage.
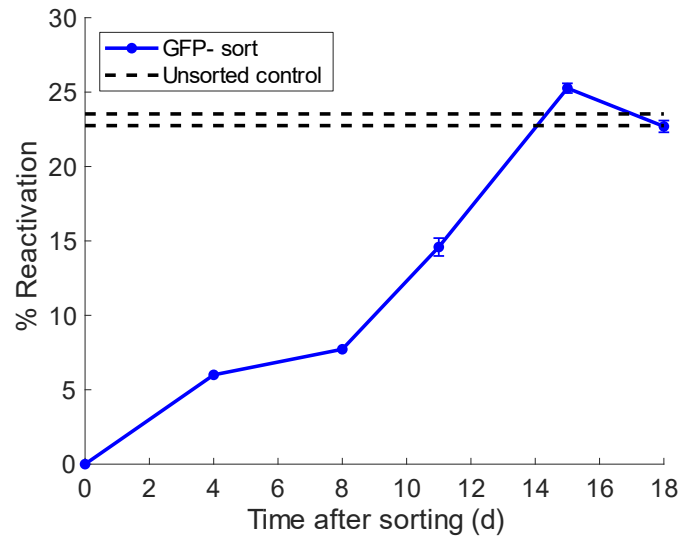
Figure S3. Recovery of % reactivation of bulk sorted irresponsive JLat 9.2 cells, Related to Figure 3. Bulk JLat 9.2 culture was treated with TNF-α for 24 hours and sorted via FACS for GFP- cells. Sorted cells were then kept in culture without TNF-α, and a sample of them were treated with TNF-α periodically, along with unsorted control. The resulting recovery curve showed a recovery time of % reactivation of about 15 days. This indicates that irresponsive JLat 9.2 cells are capable of switching into a responsive state spontaneously over time.
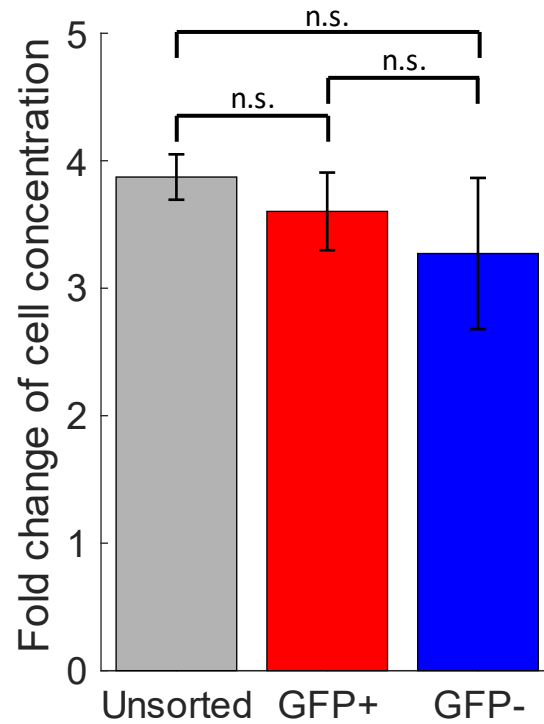
Figure S4. Growth rate of responsive and irresponsive bulk culture, Related to Figure 3.
Bulk JLat 9.2 culture was treated with TNF-α for 24 hours and sorted via FACS for GFP- cells.
Sorted cells were then kept in culture without TNF-α, and cell concentration was measured every
day. Fold changes of cell concentration were measured over courses of 3-day period for a total of
3 times (9 days total). The bars represent the average value over the three sets of measurements,
and error bars represent standard errors. Two-sample t-test yielded no significance between all
three pairs of comparison (p-values: Unsorted – GFP+: 0.488; Unsorted – GFP-: 0.387; GFP+ –
GFP-: 0.646). This suggests that JLat 9.2 cells grow at similar rates regardless of underlying cell
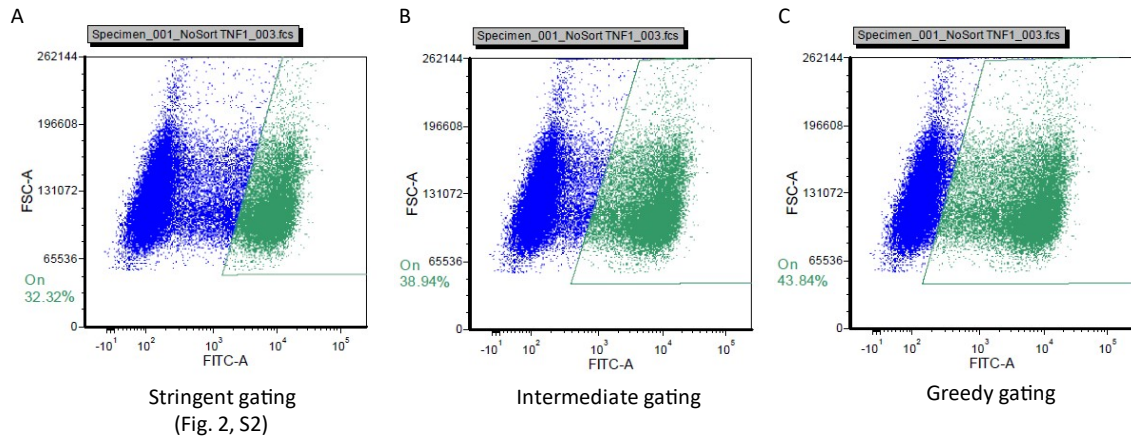states of responsiveness.

Figure S5. Gating strategies used in quantifying reactivation percentage. Related to Figure 2. (A) The stringent gating was used in analysis in Fig. 2, S2, and theoretical analyses in the main text. We explored two more styles of gating, namely **(B)** intermediate gating and **(C)** greedy gating. See Fig. S6 for analysis result with the intermediate gating and Fig. S7 for the greedy gating.
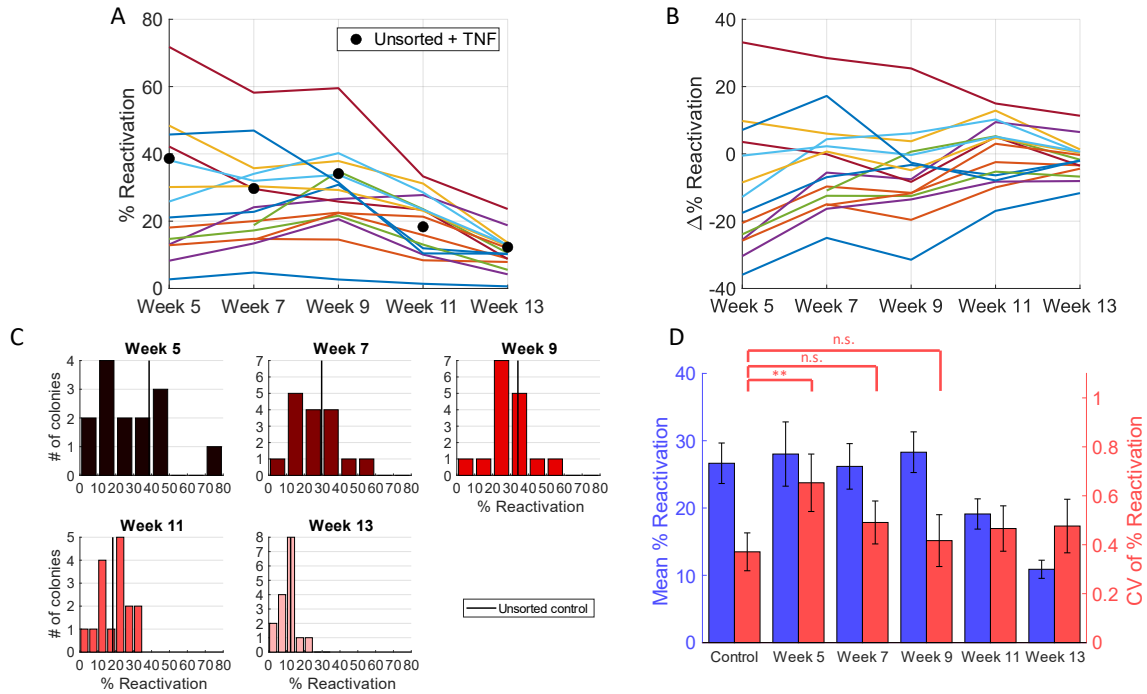
Figure S6. Analysis result using the intermediate gating strategy. Related to Figure 2. All panels displayed here show the results after the same data processing done in Fig. 2. Shifting from a stringent gating strategy (Fig. 2) to an intermediate gating strategy did not produce noteworthy changes in panels (A), (B) and (C). The statistical strength was weakened from the relaxed gating, but the difference of CV between week 5 and control stayed statistically significant.

Figure S7. Analysis result using the greedy gating strategy. Related to Figure 2. All panels displayed here show the results after the same data processing done in Fig. 2. Shifting from a stringent gating strategy (Fig. 2) to a greedy gating strategy did not produce noteworthy changes in panels (A), (B) and (C). The statistical strength was weakened from the relaxed gating, but the difference of CV between week 5 and control stayed statistically significant.
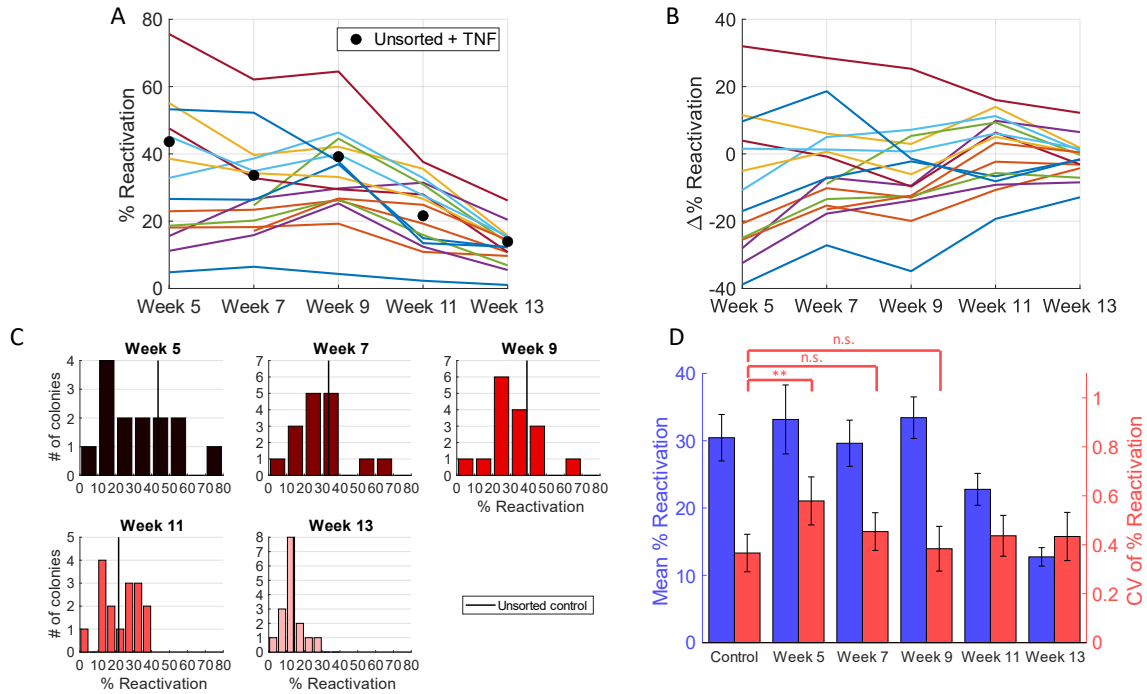
Transparent Methods

Bulk Cell Culture

JLat 9.2 cell line was obtained from the NIH AIDS Reagent Program. Bulk JLat 9.2 cells were cultured in Corning RPMI 1640 w/ L-glutamine and phenol red, with 10% fetal bovine serum (FBS) and 1% penicillin-streptomycin added. Cells were kept in T25 flasks and were passaged twice each week, with a dilution ratio of cell culture to fresh media of about 1:5.

FACS and JLat Cell Outgrowth Assay

One day before sorting, the concentration of the bulk JLat 9.2 culture was calculated using hemocytometer, and diluted to about 8×10^5 cells/ml. On the day of sorting, four V-bottom 96-well plates were prepared with 100 μl of culture media (same as the media used in bulk cell culture) and 100 μl of pure FBS. During the sorting, one cell was deposited into each well if it passed through the live gate. The plates were subsequently centrifuged to allow cells settle down to the bottom of the wells, and incubated at 37 °C, 5% CO_2. Plates were checked twice a week, and the contents of wells that turned yellow (indicates cell growth) were transferred to a 48-well plate with 1 ml of media added. After sufficient growth in 48-well plates, cells were expanded into 24-well plates with 2 ml of media, and then 6-well plates after another round of growth. See figure S1 for gating strategy during cell sorting.

Culturing Colonies Grown From Single-cells

After sufficient growth from sorted single cells, each colony was kept in culture in a 6-well plate, with 3 ml of total culture volume. Cells were passaged twice each week, with a dilution ratio of cell culture to fresh media of about 1:5.

Latency Reactivation Assay

JLat reactivation assays were conducted once every two weeks, from week 5 to week 13 post-sorting. For each colony, 1 ml of cell suspension was transferred to a well on a flat bottom 24-well plate. TNF-α was added to each well to achieve a final concentration of 10 ng/ml (Bohn-Wippert et al., 2017, Jordan et al., 2003). Afterwards cells were incubated at 37 °C, 5% CO_2 for 24 hours. Samples ran through a BD LSR Fortessa Flow Cytometry Analyzer, and data obtained was subsequently analyzed with FCS Express software. See figure S2 for gating strategy.

Statistics and Testing

We resorted to bootstrapping by creating re-samplings of the same size as the number of samples between the two sets of data under comparison. We conducted 1,000 unique re-samplings, calculating a CV and mean value for each. We counted the number of times when the re-sampled CV value of a given week is smaller than the control, and when the re-sampled mean value of a given week is larger than the control, and divide the counts by 1,000 to obtain the CV and mean p-values.

A similar procedure is used to generate standard errors that are represented as error bars in Fig. 2D. For each week's reactivation percentage data, 1,000 unique re-samplings were carried out. The standard error of a given statistic θ is calculated as the following.

$$SE(\bar{\theta}) = \sqrt{\frac{1}{n_s - 1} \sum_{i=1}^{n_s} (\bar{\theta}_{(i)} - \bar{\theta}_b)^2} \ ,$$

where n_s is the number of unique re-samplings, $\bar{\theta}_{(i)}$ is the mean of the ith re-sample, and $\bar{\theta}_b$ is the mean of all $\bar{\theta}_{(i)}$.

Mathematical Modeling

If a cell is in a responsive state at time t, i.e., $p(t) = 1$ then the probability of it switching to an irresponsive state in the infinitesimal time interval $(t, t + dt)$ is given by

$$Prob(p(t + dt) = 0 \mid p(t) = 1) = k(1 - p(t))dt \ .$$

Similarly, the probability of a switch from an irresponsive to responsive state in the infinitesimal time interval $(t, t + dt)$ is given by

$$Prob(p(t + dt) = 1 \mid p(t) = 0) = \gamma p(t)dt \ .$$

To obtain the time evolution of the first- and second-order statistical moments of $p(t)$ we use standard tools from moment dynamics that yield (Simpson et al., 2004, Soltani et al., 2015)

$$\frac{d\langle p(t) \rangle}{dt} = k - k\langle p(t) \rangle - \gamma \langle p(t) \rangle$$

$$\frac{d\langle p^2(t) \rangle}{dt} = k + \gamma \langle p(t) \rangle + k\langle p(t) \rangle - 2\gamma \langle p^2(t) \rangle - 2k\langle p^2(t) \rangle,$$

and solving these differential equations at equilibrium result in the steady-state moments given by (1). For the fluctuation test, we assume that a single cell is chosen from the original population with

$$p(0) = 1 \text{ with probability } \bar{p}$$

$$p(0) = 0 \text{ with probability } 1 - \bar{p},$$

where $\bar{p}$ is % reactivation of the original unsorted population. Given this initial random cell state, the fraction of responders $f(t)$ in the population after time t is obtained by solving the mean dynamics of $p(t)$ leading to

$$f(t) = \langle p(t) \mid p(0) \rangle = \bar{p} + e^{-(\gamma+k)t}(p(0) - \bar{p}).$$

As expected, the average % reactivation across colonies

$$\langle f(t) \rangle = \bar{p} + e^{-(\gamma+k)t}\left(\langle p(0) \rangle - \bar{p}\right) = \bar{p}$$

is the same as the average % reactivation of the original unsorted population. The coefficient of variation CV in the % reactivation is given by

$$CV^2(t) = \frac{\langle f(t)^2 \rangle - \bar{p}^2}{\bar{p}^2} = \frac{\left\langle \left(\bar{p} + e^{-(\gamma+k)t}(p(0) - \bar{p})\right)^2 \right\rangle - \bar{p}^2}{\bar{p}^2} = \frac{1 - \bar{p}}{\bar{p}}e^{-2(\gamma+k)t}$$

$$\Rightarrow CV(t) = CV_p e^{-(\gamma+k)t}, \qquad CV_p = \sqrt{\frac{1 - \bar{p}}{\bar{p}}}$$

Estimation of growth delay induced by single-cell sorting

It has been observed that using FACS to separate single cells induces stress and delays cell growth, which may contribute to the long memory timescale observed in our experiment. Here we provide an estimation of the cell growth delay from literature data. The doubling time of Jurkat cell line has been measured as around 20.7 hours (Schoene and Kamara, 1999), and has been reported to reach a saturation density of 6×10^6 cells/ml (Schneider et al., 1977). Cells used in our experiments were kept in exponential growth, combined with the assumption that exponential growth stops at half of the saturation density, it would take a healthy Jurkat cell culture about 23.1 doublings, corresponding to 478.2 hours or 2.85 weeks of growth, to expand from 1 cell to 9×10^6 cells, the maximum amount of cell in 3 ml of culture under exponential growth.

For the single-cell colonies used in our experiment, the first 14 colonies reached saturation density at about 4.5 weeks, while the rest 2 colonies reached saturation density no later than 6.5 weeks. Assuming the single cells exhibit all-or-nothing growth behaviors, stopping their growth at first before resuming normal growth with doubling time of 20.7 hours, this would correspond to a growth delay of 1.65 – 3.65 weeks.

Alternative gating strategies of quantifying experimental data

In Figure 2, we used a stringent gating to quantify reactivation percentage (Fig. S5A). To test if our result is dependent on the gating strategy, we employed two additional gating strategies, the intermediate gating (Fig. S5B) and the greedy gating (Fig. S5C). The results of the same analysis performed in Figure 2 can be found in Figure S6 for the intermediate gating and Figure S7 for the greedy gating. Of note, panels (A), (B) and (C) do not show noteworthy changes compared to Figure 2. The statistical testing strength in panel (D) is weakened by the relaxed gating (for both intermediate and greedy), but the difference of CV between week 5 and control remained statistically significant.

Mathematical modeling of the memory time scale of the responsive state yielded 2.4 weeks for the intermediate gating and 2.2 weeks for the greedy gating. These numbers are within error of our estimate using the stringent gating (2.9 ± 1.2 weeks). Thus, shifts in gating strategies do not change the main conclusions of the paper.

Supplemental References

BOHN-WIPPERT, K., TEVONIAN, E. N., MEGARIDIS, M. R. & DAR, R. D. 2017. Similarity in viral and host promoters couples viral reactivation with host cell migration. *Nat Commun,* 8**,** 15006.

JORDAN, A., BISGROVE, D. & VERDIN, E. 2003. HIV reproducibly establishes a latent infection after acute infection of T cells in vitro. *The EMBO journal,* 22.

SCHNEIDER, U., SCHWENK, H. U. & BORNKAMM, G. 1977. Characterization of EBV-genome negative "null" and "T" cell lines derived from children with acute lymphoblastic leukemia and leukemic transformed non-Hodgkin lymphoma. *Int J Cancer,* 19**,** 621-6.

SCHOENE, N. W. & KAMARA, K. S. 1999. Population doubling time, phosphatase activity, and hydrogen peroxide generation in Jurkat cells. *Free Radic Biol Med,* 27**,** 364-9.

SIMPSON, M. L., COX, C. D. & SAYLER, G. S. 2004. Frequency domain chemical Langevin analysis of stochasticity in gene transcriptional regulation. *Journal of Theoretical Biology,* 229**,** 383-394.

SOLTANI, M., VARGAS-GARCIA, C. A. & SINGH, A. 2015. Conditional Moment Closure Schemes for Studying Stochastic Dynamics of Genetic Circuits. *IEEE Trans Biomed Circuits Syst,* 9**,** 518-26.